Available online at
https://jmeche.uitm.edu.my/

e-ISSN: 2550-164X

Journal of Mechanical Engineering 23(2) 2026, 151 – 170.

Journal of Mechanical Engineering

# Structural Material Identification of Tobacco Natural Fibre Composite Panel (TNFCP) Using Stochastic Inverse Method

Nasmi Herlina Sari[1], Mohd Azmi Yunus[2*], Mimi Liza Abdul Majid[3], Mohd Shahrir Mohd Sani[4], Nurul Fatin Hamizah Ah Siak[2], Muhajir Ab Rahim[5]

[1]*Mechanical Engineering Department, Faculty of Engineering, University of Mataram, West Nusa Tenggara, Indonesia*
[2]*Structural Dynamics Analysis & Validation (SDAV), Faculty of Mechanical Engineering, Universiti Teknologi MARA, 40450 Shah Alam, Selangor, Malaysia*
[3]*Kulliyyah of Information and Communication Technology, International Islamic University Malaysia, Jalan Gombak, Malaysia*
[4]*Faculty of Mechanical and Automotive Engineering Technology, Universiti Malaysia Pahang As-Sultan Abdullah, 26600 Pekan, Pahang, Malaysia*
[5]*Faculty of Electrical Engineering and Technology, Universiti Malaysia Perlis, 02600 Arau, Perlis, Malaysia*

ARTICLE INFO

*Article history:*
Received 3 November 2025
Revised 9 April 2026
Accepted 16 April 2026
Online first
Published 15 May 2026

*Keywords:*
Composite
Stochastic
Uncertainty and variability
Modal testing
Latin hypercube sampling

*DOI:*
10.24191/jmeche.v23i2.9398

ABSTRACT

The application of natural fibre composites in structural engineering is significantly explored due to their sustainability, biodegradability, and lower environmental impact compared to synthetic fibres. Understandably, the natural composites are made from plant-based fibres and with combined polymer matrices. The natural composite is increasingly used as an alternative for lightweight and eco-friendly materials in various application industries such as automotive, aerospace, and construction industries. However, natural fibre composites are inherently heterogeneous in nature and critically influence the dynamic characteristics of the structure due to the type of fibres, the matrix material, and the fibre orientation itself. The complex interaction between these parameters of concern results in a challenge to accurately predict the mechanical properties of the composite due to the variability and uncertainty of the composite. This study proposes the structural material identification method of composite materials using a stochastic inverse method that emphasis on the uncertainty and variability of the natural tobacco fibre composite randomly generated using a Latin hypercube sampling (LHS) scheme based on an initial finite element model and experimental results of natural tobacco fibre composite. The stochastic inverse method shows a good improvement from 35.05 per cent of total error to 3.12 per cent. The proposed framework demonstrates the ability to accurately predict a range of possible material property values at a given confidence level, which can be used for structural engineering applications.

[2*] Corresponding author. *E-mail address*: mayunus@uitm.edu.my
https://doi.org/10.24191/jmeche.v23i2.9398

## INTRODUCTION

Natural fibre composites have gained significant attention as sustainable alternatives to synthetic materials in automotive, aerospace, civil, and structural engineering due to their low density, biodegradability, and favourable mechanical properties (Alsubari et al., 2021). In the automotive industry, natural fibre composites are widely used for interior panels, dashboards, and door trims because they are lightweight and recyclable, which are aligned with global efforts toward sustainable material usage. For instance, kenaf and coir fibres are already being used for automotive door and dashboard panels due to their high tensile strength and better vibration damping properties (Vanaerschot et al., 2015). Recently, tobacco fibre composites have shown a huge potential for automotive applications, owing to their high cellulose content and mechanical performance with tensile strength values making it a promising candidate for advanced composite development (Rath & Sahu, 2012; Vanaerschot et al., 2015; Nikhamkin et al., 2019).

Among numerical methods, the Finite Element Method (FEM) is widely used to predict the dynamic characteristics of structures. However, FEM is based on deterministic assumptions, in which the nominal material values used as initial input parameters are typically obtained from textbooks and the literature (Mares et al., 2004; Sulaiman et al., 2017; Aziz Shah et al., 2020; Aziz Shah et al., 2019a). Moreover, deterministic updating methods have been successfully applied to a wide range of structure systems made from isotropic materials, particularly aluminium and steel. Despite these advantages, modelling the dynamic characteristic of natural fibre composites remains a significant challenge due to various sources of uncertainties that are inherit by the structures (Sari et al., 2025). Unlike isotropic materials, natural fibre composites are heterogeneous, anisotropic, and highly sensitive to multiple interacting variables such as fibre types, orientations, stacking sequences, fibre–matrix interface quality, and manufacturing techniques, which make accurate prediction extremely difficult (Dey et al., 2017; Alsubari et al., 2021). These limitations highlight the need for advanced approaches that can capture variability and uncertainty beyond traditional deterministic modelling (Yunus et al., 2022).

The sophisticated modelling and updating strategies are explored to ensure robust and realistic representations of natural fibre composite structures between predicted and measured data. As a result, researchers have increasingly adopted nondeterministic methods such as stochastic methods, inverse approaches, and machine learning-assisted models to improve predictive accuracy and reliability of the structures (Doebling et al., 2002; Wang, 2003; Yunus et al., 2017a; Mutra et al., 2023). However, their applicability to natural fibre composites remains inconsistent, particularly due to the complexity of the natural fibre materials. On top of that, the materials exhibit intrinsic heterogeneity, moisture sensitivity, and environmental dependence, all of which introduce significant variability in dynamic responses (Shaker et al., 2008; Marwala, 2010; Aziz Shah et al., 2019b; Aziz Shah et al., 2021). This limitation highlights the need to move beyond deterministic approaches (Yaacob et al., 2019). Unlike deterministic methods, the stochastic model updating method offers an effective means of identifying unknown material properties of natural fibre composites by analysing responses such as natural frequencies, mode shapes, and damping characteristics (Yunus et al., 2017b; Pandey et al., 2025). Therefore, this study aims to develop and apply a stochastic inverse vibration-based framework for the identification of the mechanical properties of natural fibre composites.

The stochastic model can be developed by implemented probability theory that focuses on the influenced random input parameters, particularly on the input properties of the composite structure, such as Young's modulus, shear modulus, and Poisson's ratio, which are estimated by working inversely based on the measured data. In the stochastic inverse method, the measured data are served as a benchmark to update FE models through the minimization of residuals between predicted and observed results using inverse uncertainty propagation procedure (Friswell & Mottershead, 1995; Mottershead et al., 2011; Mohd Zin et al., 2017; Chen et al., 2024; Peter et al., 2019; Yunus et al., 2022). Despite these advances, the application of inverse and stochastic methods to natural fibre composites remains relatively limited, as most prior research has focused on synthetic composites or metallic structures.

https://doi.org/10.24191/jmeche.v23i2.9398

The variability in the dynamic characteristic of natural composites is strongly influenced by factors such as fibre orientation, fibre–matrix interactions, and microstructural anisotropy (Dey et al., 2017). By explicitly accounting for these sources of variability, stochastic model updating enables a more accurate representation of their mechanical response. Therefore, by incorporating randomness and uncertainty in material and structural parameters, stochastic model updating provides a more realistic and robust framework that enhances the predictive accuracy, improves confidence in structural design, and supports the wider adoption of natural fibre composites in sustainable engineering applications (Friswell & Mottershead, 1995; Zhang et al., 2023).

## METHODOLOGY

### Development of finite element model for tobacco natural fibre composite panel (TNFCP)

The tobacco natural fibre composite plate (TNFCP) with overall dimensions of length 295 mm, width 205 mm, and thickness 7 mm was modelled using 15750 CQUAD4 elements, as shown in Fig. 1. The material properties for the fibre and matrix of the natural fibre composites were assumed as orthotropic with the initial material properties of the models as tabulated in Table 1. Natural frequencies and mode shapes of the FE models were determined through the MSC NASTRAN SOL103.

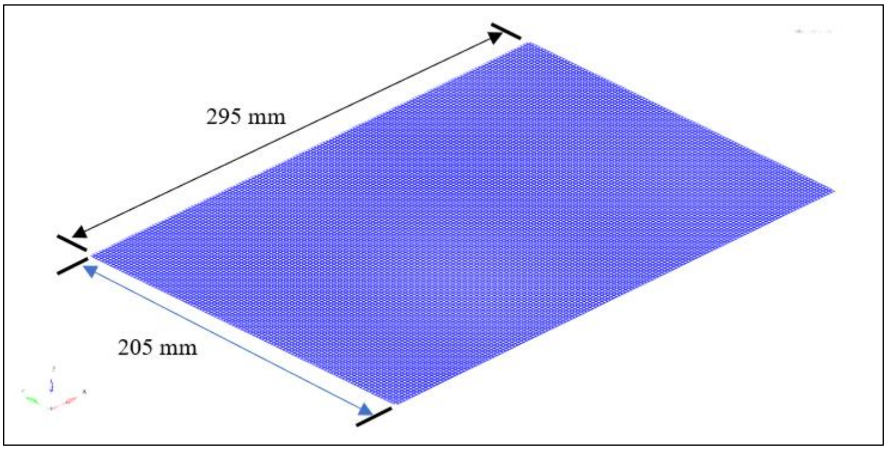


Fig. 1. Discretised FE model of tobacco composite plate.

Table 1. Initial material properties of matrix for the FE model of the composite panel (Zhang et al., 2023; Ah Siak et al., 2025)

| Properties | Values |
|---|---|
| Young's Modulus | 2550 MPa |
| Poisson's Ratio | 0.3 |
| Mass Density | 1.2e-09 tonne/mm$^3$ |

For free vibration, the following system of n differential simultaneous equilibrium is represented by Equation 1.

$$\mathbf{M}\ddot{\mathrm{U}} + \mathbf{K}\mathrm{U} = \mathrm{U} \quad (1)$$

https://doi.org/10.24191/jmeche.v23i2.9398

*M* and *K* are the properties mass and stiffness matrices, respectively, both being positive defined. Therefore, the solution of the simultaneous differential equations can be simplified as:

$$\mathbf{\ddot{U}_i\ (t) = \phi^{(i)}\ \ddot{f}_i(t)} \tag{2}$$

Substituting Equation 2 in Equation 1, to obtain:

$$\mathbf{M\phi^{(i)}\ \ddot{f}_i(t) + \ K\phi^{(i)}\ \ddot{f}_i(t) = \ 0} \tag{3}$$

Therefore, Equation 4 can be seen as:

$$\sum_{j=i}^{n} \mathbf{m_{ij}\phi_j^{(i)}\ \ddot{f}_i(t)} + \sum_{\mathbf{j=i}}^{\mathbf{n}} \mathbf{k_{ij}\phi_j^{(i)}\ f_i(t) = \ 0} \tag{4}$$

where, the solution is started with *i* and based on *n* number of modes. The values of $\omega_i$ can be presented in matrix form is:

$$\sum_{j=1}^{n} \left( \mathbf{k_{ij}} - \boldsymbol{\omega_i^2} \mathbf{m_{ij}})\boldsymbol{\phi}_j^{(i)}\right] = \mathbf{0} \tag{5}$$

$$\left([\mathbf{K}] - \boldsymbol{\omega_i^2}\ [\mathbf{M}]\right)\boldsymbol{\phi}^{(i)} \ = \ \mathbf{0} \tag{6}$$

$$\Delta = |[\mathbf{K}] - \boldsymbol{\omega_i^2}\ [\mathbf{M}] = \ \mathbf{0} \tag{7}$$

Δ is the determinant of the eigen-solution of the system. By expanding the determinant, we can obtain roots of equation in terms of natural frequencies of the system. The roots ordered are from lowest to largest natural frequency as:

$$([\boldsymbol{K}] - \boldsymbol{\omega_r^2}\ [\boldsymbol{M}])\boldsymbol{\phi}^{(r)} \ = \ \{\mathbf{0}\}\ where, \qquad r \ = \ 1, 2, \dots, n \tag{8}$$

where for each value of $\omega_{\boldsymbol{r}}$ there is a vector $^{(r)}$ known as eigenvector or vibration mode. The vector is composed of n elements $\boldsymbol{\phi}_i^{(r)}$ .

The sensitivity matrix is the derivative of the eigenvalue and eigenvector with respect to the system parameters. By calculating the derivative of the *j-th* eigenvalue, $\omega_j$, with respect to the *j-th* parameter, $\theta_j$, the eigensystems can be written as (Mottershead et al., 2011; Yunus et al., 2017a).

$$\frac{\partial \boldsymbol{\omega}_j}{\partial \theta_j} = \boldsymbol{\phi}_i^T \left(\frac{\partial \mathbf{K}}{\partial \theta_j} - \boldsymbol{\omega}_i \frac{\partial \mathbf{M}}{\partial \theta_j}\right) \boldsymbol{\phi}_i \tag{9}$$

The minimisation of natural frequencies was integrated based on the objective function as follows:

$$\boldsymbol{Z_m - Z_j = S_j\left(\theta_{j+1} - \theta_j\right)} \tag{10}$$

where $Z_m$ and $Z_j$ is the vector of measured and predicted data, respectively, the sensitivity matrix, $S_j$ and $\theta_j$ is the vector of system parameters.

The Modal Assurance Criterion (MAC) is a quantitative metric that measures the correlation between mode shapes of FE and measured structures. The MAC values vary from zero (0) to one (1), which signifies a perfect correlation between the measured and the FE mode shapes. In this case, the MAC value for each correspondence mode is expressed as follows:

https://doi.org/10.24191/jmeche.v23i2.9398

$$MAC = (\phi_{EMA}\phi_{fe}) = \frac{\left|\boldsymbol{\phi}_{EMA}^{T}\boldsymbol{\phi}_{fe}\right|^{2}}{(\boldsymbol{\phi}_{fe}^{T}\boldsymbol{\phi}_{fe})(\boldsymbol{\phi}_{EMA}^{T}\boldsymbol{\phi}_{EMA})}\ x\ 100\% \tag{11}$$

## Experimental modal analysis of TNFCP

In this study, the tobacco fibres were used as the main material for the composite panels. The fabrication of the tobacco fibres panel was done by mixing the hardener and fibre in random orientation. The mixture of resin and hardener was prepared in a weight ratio of 100: 1 and poured into a steel mould measuring 300 mm x 210 mm x 4 mm (length x width x thickness) to form the composite panel. A press machine was used to apply a pressure of 100 MPa to the mould for 20 minutes to remove the trapped air in the panel. The composite panel then had to cure for 24 hours before it was demoulded. Experiment modal analysis (EMA) or Modal testing is a method that is used by researchers to obtain the structural response of mechanical structure in terms of natural frequencies and mode shapes.

Experimental work on a tobacco natural fibres composite panel was performed in free-free boundary conditions. Data acquisition of the composite panel was performed using an impact hammer, accelerometers, and a 16-channel LMS SCADAS acquisition system. The excitation method of roving accelerometer, involving eight (8) accelerometer units, was utilised. The test was performed on the TNFCP and the accelerometers were roved around to avoid mass loading issues to the composite structure. Prior to the testing, the panel was discretised into forty-nine (49) points, and one (1) point was used as an excitation point, while another forty-eight (48) measuring points were utilised to cover all frequency of interest. In this test, only first ten (10) modes were considered based on the frequency of interest from 0 Hz to 1000 Hz and the locations of excitation and measuring points were carefully chosen in order to avoid nodal points (Sudret & Der Kiureghian, 2000). The dynamic characteristics such as natural frequencies and mode shapes of the tobacco composite structure were extracted using PolyMAX curve fitting method in LMS software. Fig. 2 shows the EMA setup of the composite panel.

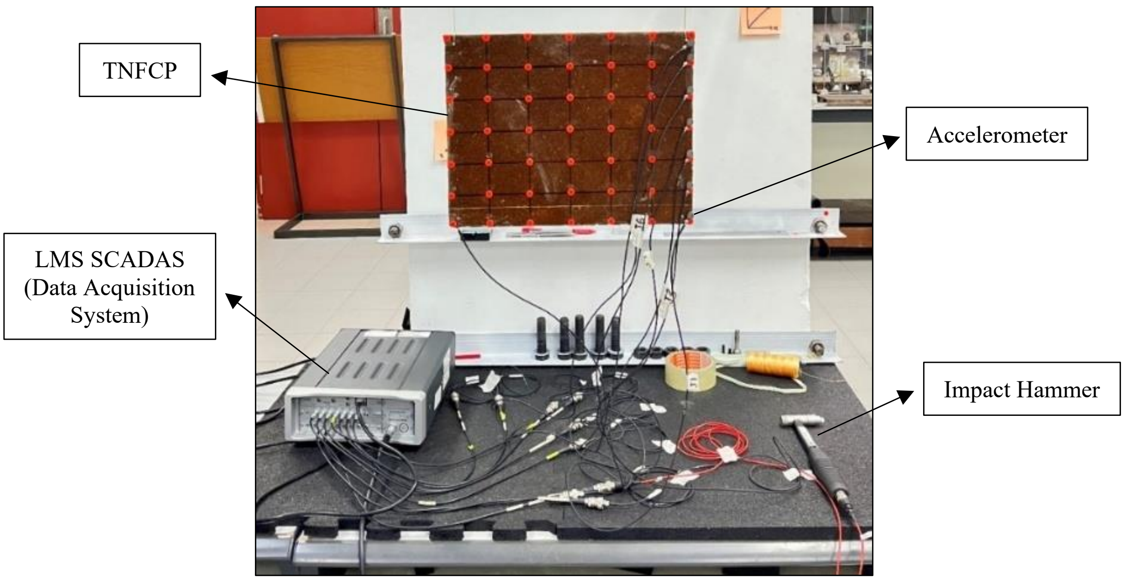


Fig. 2. Experimental set-up of TNFCP.

https://doi.org/10.24191/jmeche.v23i2.9398

### Development of an accurate stochastic model of TNFCP

The stochastic finite element method (SFEM) is a statistical tool to model structural uncertainties and randomness of a system, such as natural fibre composite structures. Understandably, the analytical model of SFEM is able to incorporate randomness in the structural parameters input, such as in geometry, boundary conditions, material properties, joint interface and properties, experimental boundary conditions and many more (Zhang et al., 2023; Zheng et al., 2024). The statistical approach of design of experiment (DoE), such as Monte Carlo Simulation (MCS), point estimate method (PEM) and Latin hypercube sampling (LHS) can be used to identify and analyse the structural inherent uncertainties and randomness of composite panels. In this paper, LHS is used for generating numerical samples by using the multidimensional distribution of system input parameters, particularly valued in uncertainty analysis due to its simplicity, versatility, and computational efficiency (Aziz Shah et al., 2021). Shaker et al. (2008) stated that the statistical parameters generated are based on mean values, variance, covariance and correlation coefficients of structural responses such as natural frequencies are used to evaluate the quality of the predicted stochastic model.

A stochastic model was developed by implementing the probability theory of LHS that focuses on the influence of random input parameters, particularly on the material properties of the composite panel. In the probability theory, a domain of random parameters, $\theta_i$ is defined as any potential values and likelihood of the random parameter being inside a certain domain is given by a Probability Density Function (PDF), $f_X(\theta_i)$(Aziz Shah et al., 2021). Furthermore, PDF can be used to evaluate the probability of likelihood of a random parameter in a specific domain of interest. For instance, if Young's modulus *($\theta_i$)* of tobacco composite is chosen as the random parameter with PDF $f_X(\theta_i)$, the probability of the parameter is defined by:

$$P(a \leq \theta_i \geq b) = \int_a^b f_X(\theta_i)dx \tag{12}$$

where $a$ and $b$ are the lower bound and the upper bound of the interval the random parameter. The probability that $\theta_i$ that falls in the interval can be written as $(a \leq \theta_i \geq b)$. After defining a variation domain of the inputs, *n* samples are then generated from a PDF over the domain. For each random sample, a the predicted of deterministic response is defined and computed using framework of FE method as stated in the subsection of development of FE Model of TNFCP. The random dynamic behaviour calculation of the SFEM principle can be expressed as:

$$([\mathbf{K}] - \boldsymbol{\omega}_r^2\ [\mathbf{M}])\boldsymbol{\phi}^{(\mathbf{r})} = \mathbf{0} \tag{13}$$

where K and M are the random stiffness and mass matrices, $\phi_i$ is the *n* x 1 modal displacement vector (mode shapes) and $\omega$ is the natural frequencies. K, M, $\phi_i$ and $\omega$ are the functions of the random parameter, $\theta_i$ in which is bounded by PDF. The mean value of natural frequencies, $\overline{\omega}$ can be calculated as:

$$([\overline{\mathbf{K}}] - \overline{\boldsymbol{\omega}}_r^2[\overline{\mathbf{M}}])\overline{\boldsymbol{\phi}}^{(\mathbf{r})} = \mathbf{0} \tag{14}$$

and the covariance of natural frequencies can be obtained by:

$$Cov(\omega_k, \omega_l) = \sum_i \sum_j \frac{\partial \overline{\omega}_k}{\partial \theta_i} \frac{\partial \overline{\omega}_l}{\partial \theta_j} Cov(\theta_i, \theta_j) \tag{15}$$

where the mean values are denoted by overbar parameters.

https://doi.org/10.24191/jmeche.v23i2.9398

To improve the accuracy of stochastic model, the stochastic model updating method (SMUM) using perturbation procedure is performed based on measured data of the composite structure. By carefully selecting the variability of input parameters in FE model, the modal parameters can be derived as follows:

$$\boldsymbol{Z_m} = \overline{\boldsymbol{Z}}_{\boldsymbol{m}} + \boldsymbol{\Delta Z_m} \tag{16}$$

$$\boldsymbol{Z_j} = \overline{\boldsymbol{Z}}_{\boldsymbol{j}} + \boldsymbol{\Delta Z_j} \tag{17}$$

$$\boldsymbol{\theta_j} = \overline{\boldsymbol{\theta}}_{\boldsymbol{j}} + \boldsymbol{\Delta\theta_j} \tag{18}$$

where, the overbar denotes as mean values and $\Delta Z_m$ and $\Delta Z_j$ are vectors of random variables. Meanwhile, variability in physical parameters at the *j-th* iteration is represented by, $\Delta\theta_j$. The stochastic model updating formulation can be rewrite by substitute Equation 16, Equation 17, and Equation 18 into Equation 10 is and defined as:

$$\widehat{\boldsymbol{\theta}}_{\boldsymbol{j+1}} + \boldsymbol{\Delta\theta_{j+1}} = \widehat{\boldsymbol{\theta}}_{\boldsymbol{j}} + \boldsymbol{\Delta\theta_j} + \left(\widehat{\boldsymbol{T}}_{\boldsymbol{j}} + \boldsymbol{\Delta T_j}\right)\left(\widehat{\boldsymbol{Z}}_{\boldsymbol{m}} + \boldsymbol{\Delta Z_m} - \widehat{\boldsymbol{Z}}_{\boldsymbol{j}} - \boldsymbol{\Delta Z_j}\right) \tag{19}$$

The transformation matrix *T* can be calculated using:

$$\widehat{\boldsymbol{T}}_{\boldsymbol{j}} = \left(\widehat{\boldsymbol{S}}_{\boldsymbol{j}}^{\boldsymbol{T}} \boldsymbol{W_{\varepsilon\varepsilon}} \widehat{\boldsymbol{S}}_{\boldsymbol{j}} + \boldsymbol{W_{\theta\theta}}\right)^{-\boldsymbol{1}} \widehat{\boldsymbol{S}}_{\boldsymbol{j}}^{\boldsymbol{T}} \boldsymbol{W_{\varepsilon\varepsilon}} \tag{20}$$

where $\hat{S}_j$ is the sensitivity matrix evaluated at mean composite parameters of the structure. $W_{\theta\theta}$ and $W_{\varepsilon\varepsilon}$ are representing the weighting matrices for selected parameters of measured data.

In this work, a number of replacement model are required. The stochastic predicted model was developed using MCS type method by implemented Latin Hypercube Sampling technique. The modelling technique was then applied to the tobacco composite panel to generate variability in the measured dynamic behaviour of the structure. The frequency covariances $\boldsymbol{f_{cov}}$ are calculated by:

$$\boldsymbol{f_{cov}} = \frac{\boldsymbol{f_\sigma}}{\boldsymbol{f_{\bar{x}}}} \tag{21}$$

where, $f_{\bar{x}}$ mean of natural frequencies and can be calculated as:

$$f_{\bar{x}} = \frac{\sum_{i=1}^{n} x_i}{n} \tag{22}$$

where, $x_i$, predicted natural frequency value for each sample and *n* is truncation order of sample generated. Standard deviation $f_\sigma$ of the natural frequencies and defined by:

$$f_\sigma = \sqrt{\frac{\sum_{i=1}^{n}(x_i - \bar{x})^2}{n-1}} \tag{23}$$

https://doi.org/10.24191/jmeche.v23i2.9398

## RESULTS AND DISCUSSION

The development of an accurate prediction and efficient model of stochastic dynamic behaviour and parameters uncertainty propagation of the TNFCP due to model source of uncertainty was the aim of this study. There are three stages involved in achieving the aim of this research. In the first stage, analytical model of the TNFCP was developed using the FEM and used to predict the natural frequencies and mode shapes of the TNFCP. The EMA natural frequencies and mode shapes were used as a benchmark to evaluate the accuracy of the initial FE model. Next for the second stage, sensitivity analysis was performed to identify the sensitive parameters to the response, and in the third stage, the model generation using the LHS method for stochastic analysis of the TNFCP was performed.

Table 2 shows the comparison of the first ten natural frequencies (10) between the EMA and initial FE model of TNFCP, with a huge discrepancy of 35.05 percent due to modelling uncertainty of the TNFCP. The representation of the natural frequency and mode shapes of initial FE model and EMA result is shown in Table 3. The MAC analysis was performed by using Equation 11, to identify the correlation between the EMA and FE mode shapes (Yaacob et al., 2019; Merzuki et al., 2022). It can be seen that, the EMA and FE mode shapes are found to have a good correlation with the MAC values more than 0.95.

Table 2. Comparison of the natural frequencies of the TNFCP between EMA, initial FE of TNFCP

| Mode Shape | EMA (Hz) | FE (Hz) | Error (%) |
|---|---|---|---|
| 1 | 95.86 | 101.06 | 5.42 |
| 2 | 119.09 | 124.87 | 4.85 |
| 3 | 213.13 | 221.10 | 3.74 |
| 4 | 229.09 | 237.35 | 3.61 |
| 5 | 276.38 | 285.78 | 3.40 |
| 6 | 349.03 | 360.15 | 3.19 |
| 7 | 441.6 | 454.79 | 2.99 |
| 8 | 461.66 | 475.25 | 2.94 |
| 9 | 577.22 | 593.76 | 2.87 |
| 10 | 628.85 | 665.43 | 5.82 |
| | | Total Error | 35.05 |

Table 3. Comparison between the initial FE and EMA mode shapes of TNFCP

| Mode | FEA | | EMA | | MAC |
|---|---|---|---|---|---|
| | Frequency (Hz) | Mode Shape | Frequency (Hz) | Mode Shape | % |
| 1 | 101.06 | 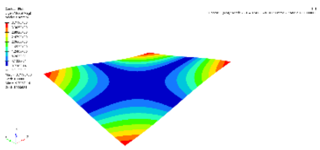 | 95.87 | 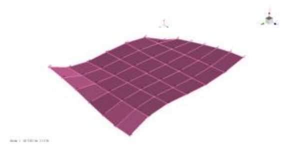 | 0.98 |
| 2 | 124.87 | 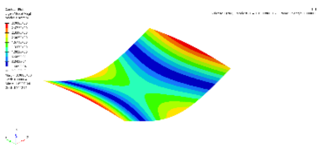 | 119.09 | 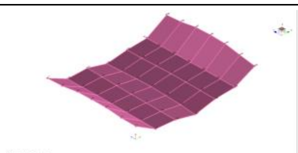 | 0.98 |

https://doi.org/10.24191/jmeche.v23i2.9398

| | | | | | |
|---|---|---|---|---|---|
| 3 | 221.10 | 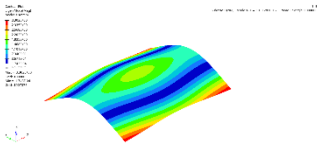 | 213.13 | 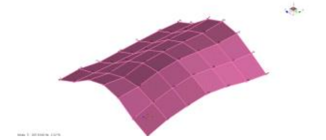 | 0.96 |
| 4 | 237.35 | 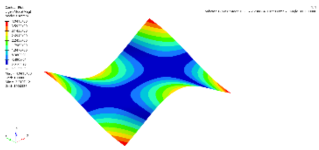 | 229.08 | 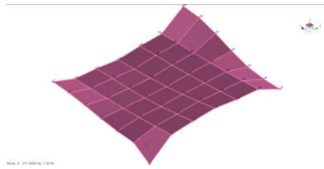 | 0.97 |
| 5 | 285.78 | 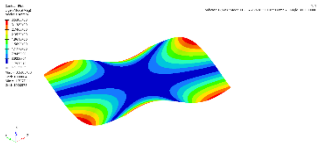 | 276.38 | 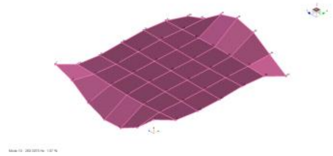 | 0.96 |
| 6 | 360.15 | 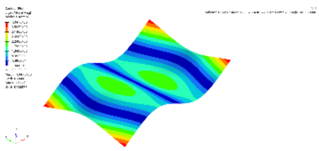 | 349.03 | 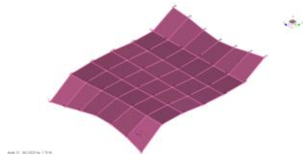 | 0.97 |
| 7 | 454.79 | 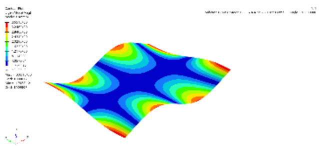 | 441.59 | 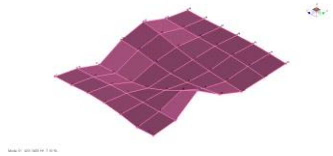 | 0.98 |
| 8 | 475.25 | 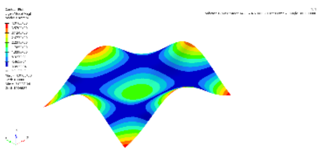 | 461.66 | 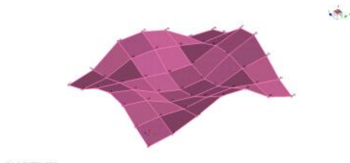 | 0.96 |
| 9 | 593.76 | 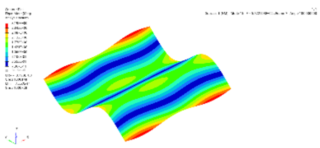 | 628.84 | 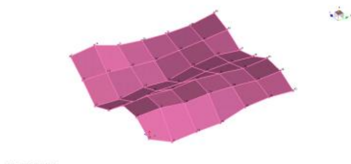 | 0.98 |
| 10 | 665.43 | 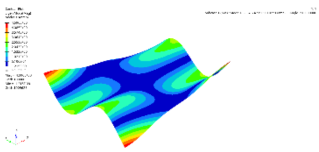 | 627.35 | 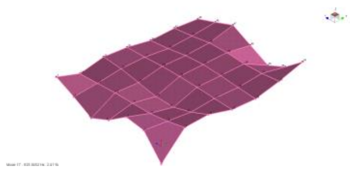 | 0.97 |

https://doi.org/10.24191/jmeche.v23i2.9398

The sensitivity analysis (Equation 9) is first used to identify the most influential input parameters of the composite panel. There are four parameters included in the sensitivity analysis, namely Young's modulus, shear modulus, Poisson's ratio, and thickness, and shown in Fig. 3. It is observed that the thickness, Young's modulus, shear modulus, and density show high sensitivity to the responses of TNFCP. Even though the thickness of the composite can be measured physically, however due to manufacturing variability the thickness of the panel is varied from 6.8 mm to 7.6 mm. Therefore, the thickness of TNFCP is included as a parameter of generated models. On the other hand, the density of the TNFCP is excluded since the weight can be measured physically. Therefore, this approach reduces parameter redundancy while preserving the essential stiffness characteristics of the panel (Aziz Shah et al., 2020; Yaacob et al., 2019).

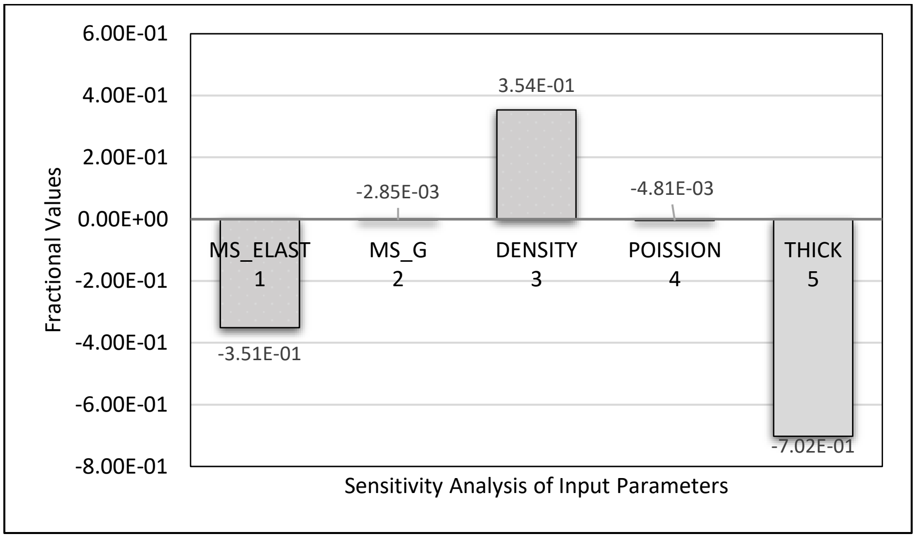


Fig. 3. Sensitivity analysis of input parameters.

To assess the effectiveness of the proposed method of stochastic FE method on the TNFCP. The LHS was used to generate the sampling data set based on design size. There are thirty (30) samples generated based on output of sensitivity analysis namely, Young's modulus (E) and thickness (t) of TNFCP.

Table 3 to Table 7 show the generated natural frequencies and material properties based on randomness of the generated models. In generating the sampling dataset, the initial values of Young's modulus and the thickness of the TNFCP were set to 2550 MPa and 7 mm, respectively. The initial values were based on the values obtained from published papers (Zhang et al., 2023; Ah Siak et al., 2025) as shown in Table 1.

https://doi.org/10.24191/jmeche.v23i2.9398

Table 3. Generated model for 30 statistical models based on the Latin Hypercube Sampling (LHS) method (Sampling model from 1 to 6)

| Mode | Exp_Freq (Hz) | NF_1 | NF_2 | NF_3 | NF_4 | NF_5 | NF_6 |
|---|---|---|---|---|---|---|---|
| 1 | 95.86 | 94.32 | 100.05 | 100.27 | 95.63 | 98.06 | 96.07 |
| 2 | 119.09 | 117.17 | 124.37 | 124.64 | 118.81 | 121.87 | 119.37 |
| 3 | 213.13 | 209.70 | 222.56 | 223.05 | 212.64 | 218.10 | 213.64 |
| 4 | 229.09 | 225.41 | 239.08 | 239.60 | 228.54 | 234.35 | 229.61 |
| 5 | 276.38 | 271.98 | 288.50 | 289.12 | 275.76 | 282.78 | 277.05 |
| 6 | 349.03 | 343.45 | 364.42 | 365.21 | 348.25 | 357.15 | 349.88 |
| 7 | 441.60 | 434.62 | 460.89 | 461.88 | 440.64 | 451.79 | 442.68 |
| 8 | 461.66 | 454.38 | 481.72 | 482.75 | 460.64 | 472.25 | 462.77 |
| 9 | 577.22 | 568.19 | 602.72 | 604.02 | 576.10 | 590.76 | 578.79 |
| 10 | 628.85 | 637.28 | 675.76 | 677.21 | 646.09 | 662.43 | 649.09 |
| Error (%) | | 15.69 | 46.98 | 49.24 | 4.77 | 26.19 | 5.39 |
| | Initial | Sample_1 | Sample_2 | Sample_3 | Sample_4 | Sample_5 | Sample_6 |
| Parameter (t) mm | 7 | 6.88 | 7.31 | 7.33 | 6.98 | 7.16 | 7.02 |
| Parameter (E) MPa | 2550 | 2622 | 2495 | 2580 | 2444 | 2546 | 2571 |

Table 4. Generated model for 30 statistical models based on the Latin Hypercube Sampling (LHS) method (Sampling model from 7 to 12)

| Mode | Exp_Freq (Hz) | NF_7 | NF_8 | NF_9 | NF_10 | NF_11 | NF_12 |
|---|---|---|---|---|---|---|---|
| 1 | 95.86 | 94.96 | 96.74 | 95.86 | 99.62 | 99.17 | 96.29 |
| 2 | 119.09 | 117.98 | 120.21 | 119.1 | 123.82 | 123.26 | 119.65 |
| 3 | 213.13 | 211.15 | 215.13 | 213.16 | 221.59 | 220.59 | 214.13 |
| 4 | 229.09 | 226.96 | 231.19 | 229.09 | 238.05 | 236.99 | 230.12 |
| 5 | 276.38 | 273.85 | 278.96 | 276.42 | 287.26 | 285.97 | 277.67 |
| 6 | 349.03 | 345.83 | 352.31 | 349.09 | 362.84 | 361.21 | 350.68 |
| 7 | 441.60 | 437.6 | 445.72 | 441.69 | 458.91 | 456.86 | 443.67 |
| 8 | 461.66 | 457.48 | 465.93 | 461.74 | 479.66 | 477.54 | 463.8 |
| 9 | 577.22 | 572.11 | 582.78 | 577.48 | 600.12 | 597.43 | 580.09 |
| 10 | 628.85 | 641.64 | 653.54 | 647.63 | 672.86 | 669.87 | 650.54 |
| Error (%) | | 10.29 | 12.33 | 3.12 | 42.45 | 37.78 | 7.65 |
| | Initial | Sample_7 | Sample_8 | Sample_9 | Sample_10 | Sample_11 | Sample_12 |
| Parameter (t) mm | 7 | 6.93 | 7.06 | 7 | 7.28 | 7.24 | 7.03 |
| Parameter (E) MPa | 2550 | 2673 | 2588 | 2605 | 2614 | 2512 | 2639 |

https://doi.org/10.24191/jmeche.v23i2.9398

Table 5. Generated model for 30 statistical models based on the Latin Hypercube Sampling (LHS) method (Sampling model from 13 to 18)

| Mode | Exp_Freq (Hz) | NF_13 | NF_14 | NF_15 | NF_16 | NF_17 | NF_18 |
|---|---|---|---|---|---|---|---|
| 1 | 95.86 | 98.29 | 98.73 | 94.75 | 99.39 | 98.51 | 95.2 |
| 2 | 119.09 | 122.16 | 122.7 | 117.71 | 123.53 | 122.43 | 118.27 |
| 3 | 213.13 | 218.62 | 219.59 | 210.67 | 221.07 | 219.1 | 211.67 |
| 4 | 229.09 | 234.89 | 235.93 | 226.45 | 237.5 | 235.41 | 227.51 |
| 5 | 276.38 | 283.44 | 284.68 | 273.22 | 286.59 | 284.06 | 274.51 |
| 6 | 349.03 | 357.99 | 359.58 | 345.04 | 362.00 | 358.79 | 346.67 |
| 7 | 441.60 | 452.84 | 454.82 | 436.61 | 457.85 | 453.83 | 438.65 |
| 8 | 461.66 | 473.35 | 475.41 | 456.44 | 478.57 | 474.38 | 458.58 |
| 9 | 577.22 | 592.14 | 594.75 | 570.80 | 598.73 | 593.44 | 573.49 |
| 10 | 628.85 | 663.97 | 666.88 | 640.18 | 671.32 | 665.43 | 643.18 |
| Error (%) | | 28.59 | 33.129 | 12.089 | 40.09 | 30.85 | 8.36 |
| | Initial | Sample_13 | Sample_14 | Sample_15 | Sample_16 | Sample_17 | Sample_18 |
| Parameter (t) mm | 7 | 7.18 | 7.21 | 6.92 | 7.26 | 7.19 | 6.95 |
| Parameter (E) MPa | 2550 | 2554 | 2648 | 2520 | 2529 | 2435 | 2486 |

Table 6. Generated model for 30 statistical models based on the Latin Hypercube Sampling (LHS) method (Sampling model from 19 to 24)

| Mode | Exp_Freq (Hz) | NF_19 | NF_20 | NF_21 | NF_22 | NF_23 | NF_24 |
|---|---|---|---|---|---|---|---|
| 1 | 95.86 | 96.97 | 96.52 | 97.40 | 99.83 | 97.18 | 98.96 |
| 2 | 119.09 | 120.49 | 119.93 | 121.04 | 124.09 | 120.77 | 122.99 |
| 3 | 213.13 | 215.64 | 214.64 | 216.61 | 222.07 | 216.13 | 220.1 |
| 4 | 229.09 | 231.74 | 230.67 | 232.77 | 238.57 | 232.25 | 236.47 |
| 5 | 276.38 | 279.62 | 278.33 | 280.87 | 287.88 | 280.24 | 285.35 |
| 6 | 349.03 | 353.15 | 351.52 | 354.73 | 363.63 | 353.94 | 360.42 |
| 7 | 441.6 | 446.77 | 444.73 | 448.75 | 459.9 | 447.76 | 455.87 |
| 8 | 461.66 | 467.03 | 464.90 | 469.09 | 480.69 | 468.06 | 476.51 |
| 9 | 577.22 | 584.16 | 581.48 | 586.77 | 601.42 | 585.47 | 596.13 |
| 10 | 628.85 | 655.08 | 652.08 | 657.99 | 674.31 | 656.53 | 668.42 |
| Error (%) | | 14.73 | 10.054 | 19.26 | 44.70 | 16.99 | 35.53 |
| | Initial | Sample_19 | Sample_20 | Sample_21 | Sample_22 | Sample_23 | Sample_24 |
| Parameter (t) mm | 7 | 7.08 | 7.05 | 7.11 | 7.29 | 7.1 | 7.23 |
| Parameter (E) MPa | 2550 | 2478 | 2427 | 2656 | 2461 | 2563 | 2537 |

In the sampling data generation, the Young's modulus and thickness of the composite panel are allowed to deviate by 20 per cent from the initial value, while the thickness was allowed to deviate by 5 per cent from the initial value to retain the physical meaning of the structure. It can be seen from sample NF 3 in Table 3 produces the highest error with a total error of 49.24 percent, and the generated value of Young's modulus and thickness of the tobacco fibre composite are 2580 MPa and 7.33 mm, respectively. In contrast, the sampling of NF 9 in Table 4 shows the most optimum model with the lowest total error of 3.12 percent in comparison to other generated samples from NF 1 to NF 30, which is consistent with previous

https://doi.org/10.24191/jmeche.v23i2.9398

nondeterministic and stochastic updating studies on uncertain structures (Aziz Shah et al., 2019; Yunus et al., 2022).

Table 7. Generated model for 30 statistical models based on the Latin Hypercube Sampling (LHS) method (Sampling model from 25 to 30)

| Mode | Exp_Freq (Hz) | NF_25 | NF_26 | NF_27 | NF_28 | NF_29 | NF_30 |
|---|---|---|---|---|---|---|---|
| 1 | 95.86 | 97.63 | 94.53 | 100.5 | 97.85 | 95.41 | 94.09 |
| 2 | 119.09 | 121.33 | 117.44 | 124.93 | 121.6 | 118.54 | 116.88 |
| 3 | 213.13 | 217.13 | 210.18 | 223.56 | 217.62 | 212.15 | 209.18 |
| 4 | 229.09 | 233.32 | 225.93 | 240.14 | 233.83 | 228.03 | 224.87 |
| 5 | 276.38 | 281.53 | 272.6 | 289.79 | 282.15 | 275.13 | 271.31 |
| 6 | 349.03 | 355.57 | 344.24 | 366.05 | 356.36 | 347.46 | 342.61 |
| 7 | 441.6 | 449.81 | 435.61 | 462.93 | 450.8 | 439.64 | 433.57 |
| 8 | 461.66 | 470.19 | 455.41 | 483.85 | 471.22 | 459.61 | 453.28 |
| 9 | 577.22 | 588.15 | 569.5 | 605.4 | 589.46 | 574.8 | 566.81 |
| 10 | 628.85 | 659.53 | 638.73 | 678.75 | 660.98 | 644.64 | 635.73 |
| Error (%) | | 21.66 | 13.89 | 51.64 | 23.93 | 6.57 | 17.60 |
| | Initial | Sample_25 | Sample_26 | Sample_27 | Sample_28 | Sample_29 | Sample_30 |
| Parameter (t) mm | 7 | 7.13 | 6.9 | 7.34 | 7.15 | 6.97 | 6.87 |
| Parameter (E) MPa | 2550 | 2452 | 2469 | 2597 | 2665 | 2503 | 2631 |

Table 8 shows the optimal results of the generated models based on the natural frequencies of TNFCP, obtained from NF9 sampling of Table 4. It can be observed from Table 8 that the structural identification using the stochastic inverse method successfully produced an improved model by reducing the initial prediction error from 35.05 percent to 3.12 percent by comparing the data from EMA, which agrees with previous inverse identification and composite model updating studies (Peter et al., 2019; Yaacob et al., 2019). Additionally, Table 9 presents the parameter variations obtained from the generated sampling dataset, and it is observed that the Young's modulus was increased from 2550 MPa to 2610 MPa, while the thickness remained unchanged at 7 mm.

Table 8. Comparison of the natural frequencies of the TNFCP between EMA, FE and updated model (NF 09)

| Mode Shape | EMA (Hz) | FE (Hz) | Error (%) | Optimised Generated FE (Hz) | Error (%) | MAC Values |
|---|---|---|---|---|---|---|
| 1 | 95.86 | 101.06 | 5.42 | 95.86 | 0.00 | 0.98 |
| 2 | 119.09 | 124.87 | 4.85 | 119.1 | 0.01 | 0.98 |
| 3 | 213.13 | 221.10 | 3.74 | 213.16 | 0.01 | 0.96 |
| 4 | 229.09 | 237.35 | 3.61 | 229.09 | 0.00 | 0.97 |
| 5 | 276.38 | 285.78 | 3.40 | 276.42 | 0.01 | 0.96 |
| 6 | 349.03 | 360.15 | 3.19 | 349.09 | 0.02 | 0.97 |
| 7 | 441.6 | 454.79 | 2.99 | 441.69 | 0.02 | 0.98 |
| 8 | 461.66 | 475.25 | 2.94 | 461.74 | 0.02 | 0.96 |
| 9 | 577.22 | 593.76 | 2.87 | 577.48 | 0.05 | 0.98 |
| 10 | 628.85 | 665.43 | 5.82 | 647.63 | 2.99 | 0.97 |
| | Total Error | | 35.05 | | 3.12 | |

https://doi.org/10.24191/jmeche.v23i2.9398

Table 9. Updated parameters for TNFCP

| Parameters | Initial | Updated (NF 9) |
|---|---|---|
| *E*, Young's Modulus | 2550 MPa | 2610 MPa |
| *t*, Thickness | 7.0 | 7.0 |

To confirm the influence of selected parameters, the Gaussian distribution plots highlight two distinct sources of uncertainty in the TNFCP based on the generated mode of thickness and Young's modulus of the TNFCP. Fig. 4(a) shows a narrow distribution centred from 6.5 mm to 7.5 mm with the mean value (μ) of 7.11 mm and the standard deviation (σ) of 0.14, that indicate low variability in the thickness of TNFCP.

In contrast, the Young's modulus of Fig. 4(b) displays a much wider distribution centred from 2300 MPa to 2800 MPa, that reflecting the variability of tobacco fibres, fibre–matrix bonding, and material heterogeneity. This high spread means that stiffness related properties contribute more significantly to the uncertainty in the panel's dynamic behaviour compared to thickness (Sari et al., 2023; Zhang et al., 2023) with the mean value (μ) of 2550.67 MPa and the standard deviation (σ) of 74.88. Table 10 and Table 11 show the statistical properties for 30 sets of sampling model configurations, namely panel thickness and Young's modulus, respectively.

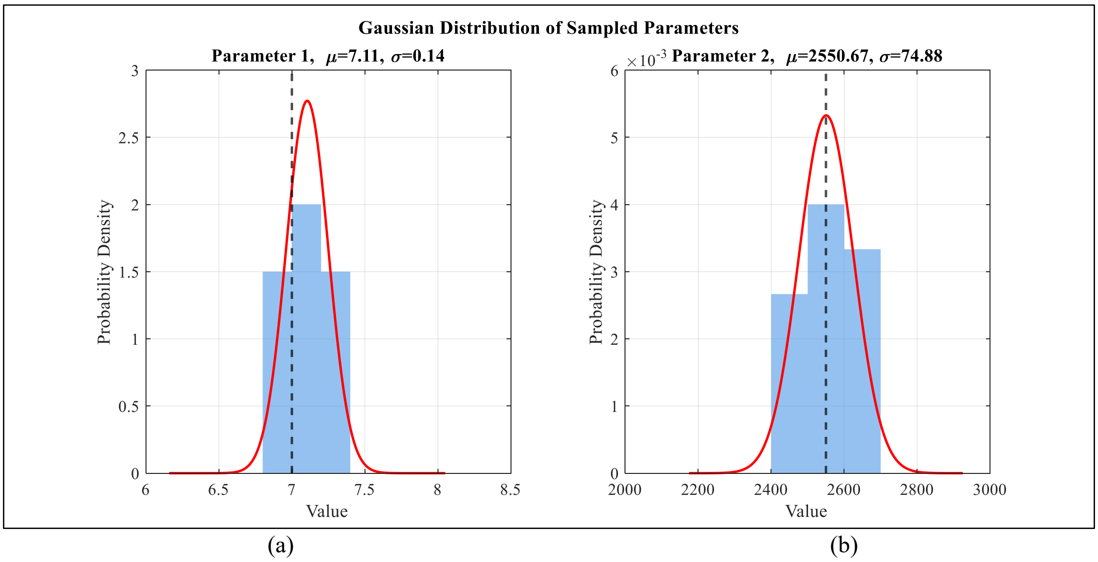


Fig. 4. Gaussian distribution of thickness (a) and Young's Modulus (b) of TNFCP.

Table 10. Statistical properties for 30 sets of sampling model configurations (Thickness)

| Parameter | Thickness, t (mm) | | | | |
|---|---|---|---|---|---|
| | Minimum, *t* min | Maximum, *t* max | Mean, $t_{\bar{x}}$ | Std. deviation, $t_{\sigma}$ | Coeff. of variation, $t_{cov}$ |
| Values | 6.87 | 7.34 | 7.11 | 0.14 | 0.02025 |

Table 11. Statistical properties for 30 sets of sampling model configurations (Young's Modulus)

| Parameter | Young's modulus, E (GPa) | | | | |
|---|---|---|---|---|---|
| | Minimum, E min | Maximum, E max | Mean, $E_{\bar{x}}$ | Std. deviation, $E_{\sigma}$ | Coeff. of variation, $E_{cov}$ |
| Values | 2427.00 | 2673.00 | 2550.67 | 74.88 | 0.02934 |

https://doi.org/10.24191/jmeche.v23i2.9398

Table 12 shows the statistical properties for 30 sets of test configurations. Based on the result of Table 12, the statistical distribution of the sampled natural frequencies for the first ten modes exhibits a consistent variation across all modes. It can be observed that the mean natural frequency increases progressively from 97.29 Hz for Mode 1 to 657.26 Hz for Mode 10, which reflects the trend of higher modes corresponding to the higher frequencies. On top of that, the tabulations of the data are represented by the standard deviation, which ranges from 1.95 Hz to 13.06 Hz. It can be said that the higher modes exhibit slightly greater absolute variability due to increased sensitivity to parameter changes, as commonly observed in vibration-based stochastic analyses and composite dynamic studies (Merzuki et al., 2022; Yunus et al., 2022).

Despite the increase in standard deviation with the number of modes, the coefficient of variation remains nearly constant at approximately 2 per cent across all modes. This indicates that the relative variability of the sampled data is uniform and well-controlled throughout the entire frequency range. The consistency in the coefficient of variation highlights the robustness of the sampling strategy and confirms that it is appropriately scaled for all modes. Furthermore, the minimum and maximum frequency bounds for each mode are approximately symmetrical approximate the mean. This data indicates that the generated sampling dataset is well balanced and free from significant bias. On top of that, the balanced distribution enhances the suitability of the dataset in capturing the inherent uncertainty of the system parameters systematically.

Table 12. Statistical properties of natural frequency for first ten modes (30 sets of test configurations)

| Mode | Natural frequency, $f_{sampling}$ (Hz) | | | | |
|---|---|---|---|---|---|
| | Minimum, $f$min | Maximum, $f$max | Mean, $f_{\bar{x}}$ | Std. deviation, $f_{\sigma}$ | Coeff. of variation, $f_{cov}$ |
| 1 | 94.09 | 100.50 | 97.29 | 1.95 | 0.02000 |
| 2 | 116.88 | 124.93 | 120.90 | 2.44 | 0.02020 |
| 3 | 209.18 | 223.56 | 216.37 | 4.36 | 0.02017 |
| 4 | 224.87 | 240.14 | 232.51 | 4.64 | 0.01994 |
| 5 | 271.31 | 289.79 | 280.55 | 5.61 | 0.01998 |
| 6 | 342.61 | 366.05 | 354.34 | 7.11 | 0.02007 |
| 7 | 433.57 | 462.93 | 448.26 | 8.91 | 0.01988 |
| 8 | 453.28 | 483.85 | 468.57 | 9.28 | 0.01980 |
| 9 | 566.81 | 605.40 | 586.12 | 11.71 | 0.01998 |
| 10 | 628.85 | 678.75 | 657.26 | 13.06 | 0.01986 |

The result in Fig. 5 demonstrates that the normalized natural frequencies of 30 samples for 10 vibration modes are close to the reference values of 1.0 across all modes indices high accuracy and consistency of the model in capturing dynamic behaviour of the structure. Moreover, the small scatter around the baseline of value of 1.0 reflects parameter-induced variability, while the slight deviation at higher modes highlights the increased sensitivity of higher-order frequencies to uncertainties in material and geometry (Yunus et al., 2022).

https://doi.org/10.24191/jmeche.v23i2.9398

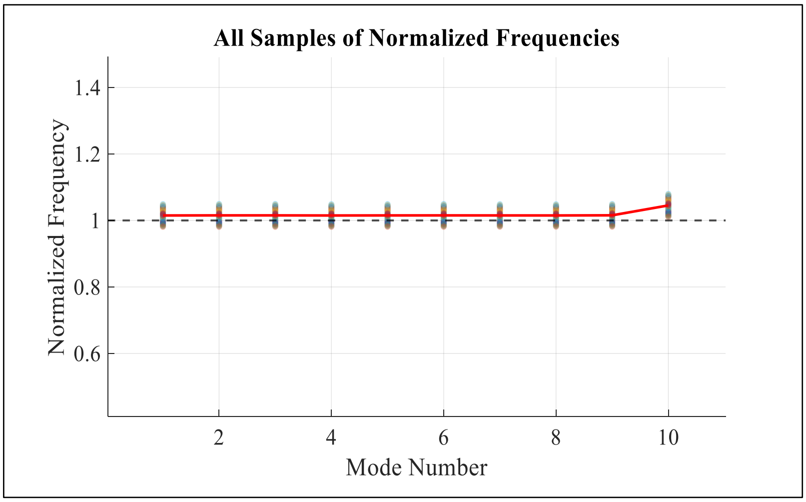


Fig. 5. The normalisation natural frequencies based on thirty (30) generated samples.

## CONCLUSIONS

This study successfully developed and validated the stochastic inverse vibration-based framework in identifying the mechanical properties and dynamic behaviour of TNFCP. By the integration of FE modelling (FEM), experimental modal analysis (EMA), and stochastic inversed methods, the research was successfully addressed the inherent uncertainties and variability present in TNFCP.

The initial material properties input of the FE model of TNFCP, initially based on deterministic assumptions. The initial FE result showed a significant discrepancy of 35.05 percent compared to the measured data. However, by implementing stochastic model replacement using Latin Hypercube Sampling (LHS), the generated model achieved remarkable accuracy as shown in SF 9 of Table 8, reducing the total error form 35.05 percent to 3.12 percent. The improvement demonstrates the robustness and reliability of the proposed stochastic framework in capturing the true dynamic characteristics of natural fibre composites.

Statistical analysis further revealed that the variability in natural frequencies was primarily influenced by the Young's modulus rather than the thickness. The Gaussian distribution and coefficient of variation analyses confirmed that material stiffness contributes more significantly to uncertainty propagation within the structure. Moreover, the normalised natural frequency plots across 30 stochastic samples indicated high model consistency and reliability, particularly for the lower vibration modes, while minor deviations at higher modes reflected natural sensitivity to input parameter uncertainties.

Overall, the proposed stochastic model updating approach proved to be an effective tool for improving the predictive accuracy and reliability of FE models of TNFCP. By incorporating the randomness and uncertainty, the developed scheme not only enhanced the confidence level of the predicted responses but also provided a more accurate representation of the dynamic behaviour of TNFCP. On top of that, the findings highlight the strong potential of stochastic inverse modelling as a robust methodology for future applications involving natural fibre composites in sustainable engineering design, particularly in automotive and structural components where accurate dynamic performance prediction is crucial.

In summary, this work establishes a reliable pathway toward more accurate and uncertainty-informed modelling of natural fibre composites, contributing significantly to the advancement of sustainable material

https://doi.org/10.24191/jmeche.v23i2.9398

research and the broader adoption of bio-based composites in high-performance structural engineering applications.

## ACKNOWLEDGEMENTS

The authors wish to acknowledge the Faculty of Mechanical Engineering, Universiti Teknologi MARA (UiTM) for providing financial support for this research. They would also like to extend their sincere gratitude for the support and help given by SDAV members.

## CONFLICT OF INTEREST STATEMENT

All authors declare that they have no conflicts of interest.

## AUTHORS' CONTRIBUTIONS

The authors confirm their contribution to the paper as follows: Mohd Azmi Yunus: investigation, validation, methodology, formal analysis, data curation, supervision writing, original draft, funding acquisition. Nasmi Herlina Sari: specimen preparation and project administration. Mimi Liza Abdul Majid: coding, data analysis, review and editing. Mohd Shahrir Mohd Sani: experiment modal analysis and editing. Nurul Fatin Hamizah Ah Siak: experimental modal analysis and editing. Muhajir Ab Rahim: data analysis and project administration. All authors reviewed the results and approved the final version of the manuscript.

## DATA AVAILABILITY/ SUPPLEMENTARY MATERIALS

All data generated or analysed during this study are included in this published article.

## ETHICS STATEMENT

The authors declare that this research did not involve human or animal subjects. All experimental procedures were performed following the institutional Safety, Health, and Environmental (HSE) protocols of Universiti Teknologi MARA (UiTM).

## REFERENCE

Ah Siak, N. F. H., Yunus, M. A., Kyprianou, A., Van Der Auweraer, H., Mohd Kahar, M. S. A., & Abdul Rani, M. N. (2025). Accurate prediction of frequency response functions of tobacco composite panel. Journal of Physics: Conference Series, 3156, 012010. https://doi.org/10.1088/1742-6596/3156/1/012010

Alsubari, S., Zuhri, M. Y. M., Sapuan, S. M., Ishak, M. R., Ilyas, R. A., & Asyraf, M. R. M. (2021). Potential of natural fiber reinforced polymer composites in sandwich structures: a review on its mechanical properties. Polymers, 13(3), 423. https://doi.org/10.3390/polym13030423

Aziz Shah, M. A. S., Yunus, M. A., Mohd Saman, A., Abdul Rani, M. N., Bahari, A. R., & Peter, C. (2019a). Finite element model updating of laser stitch welded structure. IOP Conference Series: Materials Science and Engineering, 506, 012010. https://doi.org/10.1088/1757-899X/506/1/012010

Aziz Shah, M. A. S., Yunus, M. A., Abdul Rani, M. N., Salleh, N., Wan Iskandar Mirza, W. I. I., & Peter, C. (2019b). Nondeterministic model updating of laser spot welded structure via response surface methodology. Journal of Physics: Conference Series, 1262, 012002. https://doi.org/10.1088/1742-6596/1262/1/012002

Aziz Shah, M. A. S., Yunus, M. A., & Abdul Rani, M. N. (2020). The application of design of experiment method in finite element model updating for estimating uncertainties of laser stitch welded structure. IOP Conference Series: Materials Science and Engineering, 788, 012001. https://doi.org/10.1088/1757-899X/788/1/012001

Aziz Shah, M. A. S., Yunus, M. A., Abdul Rani, M. N., Omar, R., & Mora, A. (2021). Stochastic model updating of bolt-jointed structure for structural dynamics applications. International Journal of Automotive and Mechanical Engineering, 18(2), 8760–8771. https://doi.org/10.15282/ijame.18.2.2021.14.0670

Aziz Shah, M. A. S., Yunus, M. A., Abdul Rani, M. N., & Yahya, Z. (2022). Stochastic study on dynamic behaviour of bolted joint structure. AIP Conference Proceedings, 2545(1), 020009. https://doi.org/10.1063/5.0103291

Chen, Y., Zhong, R., Wang, Q., Chen, L., & Qin, B. (2024). Uncertain stochastic vibration characteristic analysis of composite laminated rectangular plate based on improved kriging model. Composite Structures, 340, 118180. https://doi.org/10.1016/j.compstruct.2024.118180

Dey, S., Mukhopadhyay, T., & Adhikari, S. (2017). Metamodel-based high-fidelity stochastic analysis of composite laminates: a concise review with critical comparative assessment. Composite Structures, 171, 227–250. https://doi.org/10.1016/j.compstruct.2017.01.061

Doebling, S. W., Hemez, F. M., Schultze, J. F., & Cundy, A. L. (2002). A metamodel-based approach to model validation for nonlinear finite element simulations. Proceedings of IMAC XX (pp. 1-8). Los Alamos National Laboratory.

Friswell, M. I., & Mottershead, J. E. (1995). Finite element model updating in structural dynamics. Springer. https://doi.org/10.1007/978-94-015-8508-8

Mares, C., Mottershead, J. E., & Friswell, M. I. (2004). Stochastic model updating of a spot welded structure. Proceedings of ISMA 2004: International Conference on Noise and Vibration Engineering (pp. 1885–1898). Katholieke Universiteit Leuven, Belgium.

Marwala, T. (2010). Finite element model updating using computational intelligence techniques. Applications to structural dynamics. Springer.

Merzuki, M. N. M., Ma, Q., Rejab, M. R. M., Sani, M. S. M., & Zhang, B. (2022). Experimental and numerical investigation of fibre-metal-laminates (FMLs) under free vibration analysis. Materials Today: Proceedings, 48(4), 854–860. https://doi.org/10.1016/j.matpr.2021.02.409

Mohd Zin, M. S., Abdul Rani, M. N., Yunus, M. A., Wan Iskandar Mirza, W. I. I., Mat Isa, A. A., & Mohamed, Z. (2017). Modal and FRF based updating methods for the investigation of the dynamic behaviour of a plate. Journal of Mechanical Engineering, 4(3), 175–189.

https://doi.org/10.24191/jmeche.v23i2.9398

Mottershead, J. E., Link, M., & Friswell, M. I. (2011). The sensitivity method in finite element model updating: a tutorial. Mechanical Systems and Signal Processing, 25(7), 2275–2296.

Mutra, R. R., Reddy, D. M., Amarnath, M., Abdul Rani, M. N., Yunus, M. A., & Sani, M. S. M. (2023). Artificial neural network-based fault diagnosis of gearbox using empirical mode decomposition from vibration response. International Journal of Automotive and Mechanical Engineering, 20(3), 10695–10709. https://doi.org/10.15282/ijame.20.3.2023.12.0826

Nikhamkin, M. S., Semenov, S. V., & Solomonov, D. G. (2019). Application of experimental modal analysis for identification of laminated carbon fiber-reinforced plastics model parameters. Proceedings of the 4th International Conference on Industrial Engineering (pp. 487–497). Springer International Publishing. https://doi.org/10.1007/978-3-319-95630-5_51

Pandey, P., Jamia, N., Chatterjee, T., Khodaparast, H. H., & Friswell, M. I. (2025). Modelling and stochastic updating of nonlinear structural joints. Mechanical Systems and Signal Processing, 232, 112697. https://doi.org/10.1016/j.ymssp.2025.112697

Peter, C., Abdul Rani, M. N., Yunus, M. A., Mohd Zin, M. S., Kalam, A., & Aziz Shah, M. A. S. (2019). Inverse method for material properties identification of a kenaf reinforced composite. AIP Conference Proceedings, 2059(1), 020058. https://doi.org/10.1063/1.5086001

Rath, M. K., & Sahu, S. K. (2012). Vibration of woven fiber laminated composite plates in hygrothermal environment. Journal of Vibration and Control, 18(13), 1957-1970.

Sari, N. H., Sujita, Suteja, Firdaus, M., Wardani, D., & Syafri, E. (2025). Enhancement of physical, mechanical, thermal, and dynamic mechanical properties of polyester composites using alkali-engineered tobacco stem particles. Discover Materials, 5(1), 190. https://doi.org/10.1007/s43939-025-00388-3

Sari, N. H., Syafri, E., Suteja, Fatriasari, W., & Karimah, A. (2023). Comprehensive characterization of novel cellulose fiber from Paederia foetida and its modification for sustainable composites application. Journal of Applied Science and Engineering, 26(10), 1399–1408. https://doi.org/10.6180/jase.202310_26(10).0005

Shaker, A., Abdelrahman, W. G., Tawfik, M., & Sadek, E. (2008). Stochastic finite element analysis of the free vibration of laminated composite plates. Computational Mechanics, 41(4), 493–501. https://doi.org/10.1007/s00466-007-0205-7

Sudret, B., & Der Kiureghian, A. (2000). Stochastic finite element methods and reliability. A state-of-the-art report (Report No. UCB/SEMM-2000/08). University of California, Berkeley.

Sulaiman, M. S. A., Yunus, M. A., Abdul Rani, M. N., Mohd Saman, A., Mohamed, Z., & Aziz Shah, M. A. S. (2017). Characterisation of the dynamic characteristics of a complex jointed structure. MATEC Web of Conferences, 108, 12001. https://doi.org/10.1051/matecconf/201710812001

Vanaerschot, A., Lomov, S., Moens, D., & Vandepitte, D. (2015). Variability in composite materials properties. Applied Mechanics and Materials, 807, 23–33. https://doi.org/10.4028/www.scientific.net/amm.807.23

Wang, G. G. (2003). Adaptive response surface method using inherited Latin hypercube design points. Journal of Mechanical Design, 125(2), 210–220. https://doi.org/10.1115/1.1561044

Yaacob, R. M., Hashim, M. A. H., & Sani, M. S. M. (2019). Finite element modeling and updating of the composite plate structure. Journal of Physics: Conference Series, 1262, 012013. https://doi.org/10.1088/1742-6596/1262/1/012013

https://doi.org/10.24191/jmeche.v23i2.9398

Yunus, M. A., Aziz Shah, M. A. S., Abdul Rani, M. N., Wan Iskandar Mirza, W. I. I., & Kushairi, S. (2017a). Experimental and finite element analysis of laser stitch welded structure. Journal of Mechanical Engineering, 4(3), 155–162.

Yunus, M. A., Nazri, S., Abdul Rani, M. N., Tormodi, A., & Kasolang, S. (2017b). Response surface reconciliation method of bolted joints structure. MATEC Web of Conferences, 90, 01013.

Yunus, M. A., Aziz Shah, M. A. S., & Abdul Rani, M. N. (2022). Uncertain parameters estimation using multi-dimensional analysis and stochastic model updating. International Journal of Automotive and Mechanical Engineering, 19(1), 9498–9508. https://doi.org/10.15282/ijame.19.1.2022.13.0732

Zheng, Z., Beer, M., & Nackenhorst, U. (2024). Efficient stochastic modal decomposition methods for structural stochastic static and dynamic analyses. International Journal for Numerical Methods in Engineering, 125(12), e7469. https://doi.org/10.1002/nme.7469

Zhang, X., Zhu, X., Duan, J., Li, H., Xu, L., Xiong, L., Luo, Q., Yang, M., & Chang, X. (2023). Comparative study on properties of polypropylene-based composites reinforced with tobacco stalk fibers (unmodified/modified) from different parts of tobacco stalk. Industrial Crops and Products, 201, 116890. https://doi.org/10.1016/j.indcrop.2023.116890



https://doi.org/10.24191/jmeche.v23i2.9398